

Imino Proton Exchange in the 5S RNA of *Escherichia coli* and Its Complex with Protein L25 at 490 MHz[†]

Neocles B. Leontis[‡] and Peter B. Moore*

Department of Chemistry, Yale University, New Haven, Connecticut 06511

Received January 14, 1986; Revised Manuscript Received May 8, 1986

ABSTRACT: Imino proton exchange has been examined by NMR in the 5S RNA of *Escherichia coli*, its principal RNase A resistant fragment, fragment 1 (bases 1-11, 69-120), and complexes between that fragment and ribosomal protein L25 by using both real-time and relaxation techniques. Fragment 1 RNA imino protons exchange at rates between 0.5 and 15 s⁻¹ at 303 K in 5 mM cacodylate buffer, pH 7.4. In contrast with many tRNAs, intact 5S RNA contains no imino protons with exchange lifetimes as great as 1 min. Consistent with the results of Gueron and his colleagues [Leroy, J. L., Bolo, N., Figueroa, N., Plateau, P., & Gueron, M. (1985) *J. Biomol. Struct. Dyn.* 2, 915-939; Leroy, J. L., Broseta, D., & Gueron, M. (1985) *J. Mol. Biol.* 184, 165-178] with tRNA, exchange in 5S RNA is catalyst-limited under conditions generally used for imino proton spectroscopy, such as those given above. Using Gueron's catalyst saturation technique, base pair opening rates have been measured for several AU and GU base pairs in fragment 1. They range from 50 to 300 s⁻¹ at 303 K and depend on base pair type and also to some degree on context. Similar studies have been done on complexes of L25 and fragment 1. The binding of L25 to fragment 1 reduces the exchange rate of many imino protons within the region to which it binds, consistent with the hypothesis that its binding stabilizes the secondary structure of 5S RNA.

The downfield resonances of the proton NMR spectrum of a nucleic acid represent base imino protons protected from solvent exchange by hydrogen bonding (Kearns & Shulman, 1974). Assignment of that portion of the spectrum identifies the nucleic acid's secondary structure, and proton exchange studies done on the same resonances can provide information on its dynamics.

Below we report the results of hydrogen-exchange experiments done on the imino protons of the 5S RNA of *E. coli* and its fragment 1 moiety (bases 1-11, 69-120) by NMR methods. Unlike many tRNAs, intact 5S RNA contains no imino protons with exchange lifetimes of the order of minutes or greater [see Leroy et al. (1985a)]. Furthermore, exchange is catalyst-limited for many base-paired imino protons within the fragment 1 portion of 5S RNAs under the ionic conditions commonly used to observe the downfield spectrum of nucleic acids (e.g., 5 mM cacodylate, phosphate, or HEPES,¹ pH 7, 0.1 M NaCl). This finding is in agreement with observations made by Gueron and his colleagues on synthetic RNAs and on tRNAs (Leroy et al., 1985a,b). In the presence of saturating levels of base catalyst, when exchange is open-limited, the AU and GU imino protons in 5S RNA exchange 10-30 times faster than they do under "standard" NMR conditions.

Catalyst saturation experiments done on the complex between fragment 1 and ribosomal protein L25 show that protein binding reduces the opening rates of some base pairs within the protein binding site 2- to 3-fold. The resonances of other imino protons within the binding site become unresponsive to added catalyst, suggesting that the opening times of the base

pairs to which they belong become too slow to measure when the protein is bound. Not all base pairs in the binding site respond in this way, however. The exchange properties of some are unaltered by protein binding.

THEORY

Imino proton exchange in nucleic acids is base catalyzed, and occurs only when imino protons are exposed to solvent, i.e., when they are not involved in intramolecular hydrogen bonding [see Englander & Kallenbach (1983)]. The analysis of Eigen (1964) shows that the rate of exchange of an exposed imino proton, $k_{tr(transfer)}$, is given by

$$k_{tr} = \alpha D[B](1 + 10^{-\Delta pK})^{-1} \quad (1)$$

where α is an accessibility factor, D is the diffusional rate constant describing the encounter of an imino proton with molecules of base, $[B]$ the concentration of base, and ΔpK the difference in pK between the base responsible for catalysis and the nucleotide imino proton in question. For nucleotides in solution, α is defined as 1.0. If the placement of a nucleotide in a nucleic acid makes exchange of its imino proton, when exposed to solvent, less efficient than it is for free nucleotides, α will be less than 1.0. For free nucleotides, D is of the order of $10^{10} \text{ M}^{-1} \text{ s}^{-1}$. The pK 's of nucleotide imino protons are about 9.3, and those of polynucleotides are similar (Aylward, 1967). The predictions of eq 1 have been verified experimentally for free nucleotides (Fritzsche et al., 1981).

The exchange rate for an imino proton in a base pair, $k_{ex(change)}$, is k_{tr} multiplied by the fraction of the time that the base pair is open to permit solvent access. Following Leroy et al. (1985a)

$$\tau_{ex} = 1/k_{ex} = (1/k_{op})(1 + k_{cl}/k_{tr}) \quad (2)$$

* This work was supported by a grant from the National Institutes of Health (GM32206). The 490-MHz NMR spectrometer at Yale is supported by a grant from the NIGMS Shared Instrumentation Program (GM32243-02S1).

* Address correspondence to this author.

[†] Present address: Department of Chemistry, Bowling Green University, Bowling Green, OH 43403. This work forms part of a dissertation submitted to the Graduate School of Yale University in partial fulfillment of the requirements for the Ph.D. degree.

¹ Abbreviations: NMR, nuclear magnetic resonance; ADA, alternate delay accumulation; EDTA, ethylenediaminetetraacetic acid; HEPES, *N*-(2-hydroxyethyl)piperazine-*N'*-2-ethanesulfonic acid; MES, 2-(*N*-morpholino)ethanesulfonic acid; Tris, tris(hydroxymethyl)aminomethane.

where τ_{ex} is the exchange time of a given imino proton, $k_{\text{op(en)}}$ is the rate at which the closed base pair opens, and $k_{\text{cl(ose)}}$ is the rate at which the base pair closes, once opened. Defining $[B_{\text{eq}}]$ as the concentration of base necessary to make $k_{\text{tr}} = k_{\text{cl}}$ (see eq 1) and τ_{op} as $1/k_{\text{op}}$, eq 2 can be written

$$\tau_{\text{ex}} = \tau_{\text{op}}(1 + [B_{\text{eq}}]/[B]) \quad (3)$$

In the event that $[B]$ is large compared to $[B_{\text{eq}}]$, the exchange rate will equal k_{op} , a quantity of interest in connection with the dynamics of nucleic acid structures. The closing rate, k_{cl} , cannot be determined from exchange data alone because they do not permit the independent estimation of α and D .

The simplest way to measure imino proton exchange by NMR is to follow the disappearance of resonances as a function of time after the introduction of a protonated sample into D_2O [e.g., Leroy et al. (1985a)]. The time needed to introduce samples into D_2O and acquire spectra restricts this method to the measurement of exchange times greater than a few minutes.

Exchange processes occurring on faster time scales can be measured by NMR because exchange contributes to the relaxation of imino proton resonances. Recently Gueron and his colleagues have devised a technique for measuring base pair opening times which depends on the sensitivity of exchange to catalyst concentration (Leroy et al., 1985a,b). The spectrum of a sample is collected in buffers containing increasing concentrations of base catalyst (e.g., Tris or imidazole), and the widths of its imino proton resonances are measured at half-height. The full width at half-height of a resonance times π gives its effective spin-spin relaxation rate. Provided the opening rate for the base pair with which an imino proton is associated is appreciable compared to the relaxation rate, $(1/T_2)$, eq 3 predicts that its resonance should broaden measurably as the base concentration increases. The incremental change in T_2 is an indication of τ_{ex} , the exchange time for the resonance. Plots of the reciprocal of τ_{ex} vs. $1/[B]$ should be linear, and extrapolation of τ_{ex} to $1/[B]$ equals zero provides an estimate for τ_{op} , the lifetime of the closed state of the base pair in question.

T_1 measurements can also give information about exchange. The spin system of the nucleic acid is prepared by using an appropriate pulse sequence so that the imino proton resonances are either saturated or inverted, while water protons are unperturbed. [For a discussion of the effect different methods for preparing the spin systems of a molecule have on the T_1 s which are observed, see Kearns (1983).] Exchange taking place after the preparation of the spin system will replace inverted (or saturated) imino protons with uninverted (or unsaturated) water protons, accelerating the relaxation of the imino proton resonances back to the equilibrium state. In principle one could make T_1 measurements on a sample as a function of catalyst concentration and analyze the data as just described for T_2 measurements.

NOE experiments done on ^{19}F -labeled 5S RNA have demonstrated that the correlation time of the molecule is of the order of 10^{-8} s or larger, consistent with the view that rigid body rotations dominate its magnetic relaxation processes (Marshall & Smith, 1980). The rotational correlation time of a rigid molecule (τ_c) is proportional to viscosity/ T (Cantor & Schimmel, 1980). Furthermore, the longitudinal relaxation rate $(1/T_1)$ of a selectively inverted or saturated proton resonance is proportional to correlation time provided $(\omega\tau_c)^2$ is large compared to 1, as it clearly is in this case ($\omega = 2\pi 500$ MHz) (Kearns, 1983). Since the correlation time should fall as temperature increases, T_1 should rise, provided magnetic processes control relaxation. The exchange process, on the

other hand, accelerates with temperature following the Arrhenius equation, and exchange accelerates relaxation. Thus at low temperatures, the longitudinal relaxation time of an imino proton resonance should increase with increasing temperature, but at some point, when exchange begins to dominate, it should start decreasing sharply with temperature. Plotted as the logarithm of the relaxation rate vs. (absolute temperature) $^{-1}$, the high-temperature data should give a straight line, the slope of which is proportional to the activation energy for the exchange process. Once the high-temperature trend is known, the exchange rate can be estimated at any temperature by extrapolation. Data demonstrating this response of the T_1 s of nucleic acid imino protons to changes in temperature may be found elsewhere [e.g., Hurd & Reid (1980), Tropp & Redfield (1983), Kearns (1983), Patel et al., (1985), Mirau et al. (1985)].

MATERIALS AND METHODS

5S RNA and Fragment 1. The 5S RNA used for all experiments was the *rrnB* gene product obtained from the overproducing strain HB101/pKK5-1 (Brosius, 1984). The methods used for overproduction and isolation of the 5S RNA from this strain have been described previously (Kime & Moore, 1983b). The *rrnB* gene product differs from the consensus *E. coli* sequence in having an A at position 12 rather than a C. The overproduced material is not fully matured; it has a few extra bases at both its 3' and 5' ends (Kime et al., 1984). Fragment 1 was prepared by limited digestion with RNase A followed by purification on Sephadex G-100 (Kime & Moore, 1983a).

L25 and L25-RNA Complexes. L25 was prepared from ribosomes as described before (Kime et al., 1981; Kime & Moore, 1982). The purified protein, which is stored in urea at 200 K, was dialyzed into 5 mM cacodylic acid, pH 7.2, 4 mM $MgCl_2$, 0.1 M KCl, and the buffer used for complex formation and spectroscopy. The concentration of the protein was estimated from its extinction coefficient at 276 nm by using 0.38 as the absorbance of a 0.1% solution of this protein. Complexes were formed by adding a 5% molar excess of L25 to solutions of RNA at concentrations around 0.1 mM at 298 K.

NMR Methods. Spectra were collected on the 490-MHz NMR spectrometer at the Yale Chemical Instrumentation Center. Samples were made up in solvents containing 5% D_2O to permit the spectrometer lock to function. Except where otherwise stated, all samples were equilibrated at the buffer conditions stated by dialysis, and RNA concentrations of about 1 mM were achieved by ultrafiltration following dialysis. All samples contained dioxane at 2 mM to serve as a chemical shift standard. The chemical shift of dioxane relative to that of the methyl resonance of 3-(trimethylsilyl)-1-propanesulfonic acid was taken to be 3.741 ppm at all temperatures.

Sample temperatures were controlled by using a Bruker B-ST 100/700 temperature control unit. The chemical shift difference between HDO and dioxane varies nearly linearly with temperature over the range of temperatures explored in this work. As judged by HDO-dioxane chemical shift differences, the temperature controller replicated temperatures from one run to the next to with an accuracy of better than 0.5 K, consistent with the manufacturer's specifications for the unit.

The spectrometer was routinely shimmed so as to make the full width at half-height of the dioxane proton peaks in each sample less than 2 Hz. Given that the full widths at half-maximum of the downfield resonances of the RNAs studied here exceed 15 Hz in all cases, the contribution made by

spectrometer inhomogeneity to the resonance widths observed is modest.

Real-Time Exchange of Imino Protons. A sample of rrnB 5S RNA was dialyzed into a buffer containing 5 mM sodium cacodylate, pH 6.0, 5 mM MgCl₂, 0.1 M KCl, and 0.5 mM EDTA (added to buffer paramagnetic ions) and then concentrated to 150 mg/mL (based on optical density using $20A_{260\text{nm}} = 1 \text{ mg/mL}$). The sample was divided into two portions of 0.150 mL. The first portion was diluted to 40 mg/mL with dialysis buffer and then used to shim the spectrometer and acquire reference spectra. The second portion was diluted 3:1 with dialysis buffer prepared in D₂O and immediately placed in the spectrometer. The first spectrum was accumulated in 1 min (pulse recycle time 0.2 s) within 3 min of diluting with D₂O buffer.

T_1 Relaxation Times. T_1 relaxation times of imino protons were measured by the method of inversion recovery. The imino proton region (10–15 ppm) was semiselectively inverted by using a $90^\circ - \tau - 90^\circ$ composite 180° pulse in which the delay, τ , was adjusted to avoid excitation of the solvent (water) resonance (Kime & Moore, 1983c). The transmitter offset was placed in the middle of the imino region in order to invert the imino region as uniformly as possible. Spectra were accumulated following a variable delay, using a $45^\circ - \tau - 45^\circ$ observation pulse sequence in combination with ADA (Roth et al., 1980) to suppress the solvent resonance. In a typical run, spectra were collected in an interleaved fashion for 19 different delay times varying from 1 to 500 ms. A relaxation decay of 1 s was included in each cycle. A twentieth spectrum, collected without the initial inversion pulses, served as the fully relaxed reference spectrum. Spectra were subjected to exponential-to-Gaussian multiplication prior to Fourier transformation to facilitate determination of base lines. The logarithm of the difference in resonance amplitude between that observed in the fully relaxed spectrum and that seen in the spectrum taken with a delay time of t was plotted vs. t for each resonance. Relaxation times were calculated from the initial slopes of the resulting semilog plots.

T_1 Data Analysis. The magnetic and exchange components of the T_1 relaxation of each resonance were estimated by fitting the data to the model for the temperature dependence of relaxation suggestion above

$$k_c = k_m \eta(T)/T + k_{ex} \exp(-\Delta H/RT) \quad (4)$$

k_c is the calculated value for the overall relaxation rate. $k_m \eta(T)/T$ is the relaxation rate due to magnetic processes which is taken to be a constant, k_m , times the viscosity of water, $\eta(T)$, divided by the temperature. $k_{ex} \exp(-\Delta H/RT)$ is the exchange contribution to relaxation rate, where ΔH is the activation energy for the exchange process and k_{ex} the exchange rate at infinite temperature.

Values for the adjustable parameters in eq 4 were estimated for each resonance by using an iterative, nonlinear, least-squares program based on Newton's method (Bard, 1974). The objective function was $[(k_c(T) - k_{ob}(T))/k_{ob}(T)]^2$ summed over the set of observations for a given resonance. k_{ob} is the observed relaxation rate ($=1/T_1$). This choice of objective function leads to minimization of the percentage deviation of k_c from k_{ob} averaged over the whole set of observations. The initial value for k_m was estimated by assuming that the relaxation observed at the lowest temperature in a series is due entirely to magnetic processes. To obtain initial values for k_{ex} and ΔH , the two highest temperature data points were analyzed assuming that their relaxation was entirely due to exchange. Refinement of these initial estimates converged rapidly. The residuals obtained upon convergence are con-

sistent with the view that individual measurements of T_1 had standard errors of about 10%. Errors for parameters were calculated on that basis.

Base-Catalyzed Imino Proton Exchange. Samples of fragment 1 were prepared in 0.5 mM Tris buffer at pH 7.5, 5 mM MgCl₂, and 100 mM KCl. L25-fragment 1 samples were prepared in 5 mM cacodylate, as described above. (The spectrum of fragment 1 in 0.5 mM Tris is similar to that in 5 mM cacodylate at the same pH.) Tris- d_{11} was added to the NMR sample from a 1 M stock solution adjusted to pH 7.4. Spectra were accumulated at each Tris concentration at 293, 303, and 313 K in the case of the RNA sample but only at 303 K in the case of the L25-RNA complex. A relaxation delay of 1.0 s preceded each scan.

Spectra were plotted on a horizontal scale of 0.1 ppm/cm (5 Hz/mm), and line widths were determined at half-height with a ruler. The errors for the widths at half-height were calculated for each resonance from estimates of the uncertainties in the position of the base line and of the width measurement itself. Assuming resonance shapes are Lorentzian, $\Delta v_{1/2}$, the full width at half-height is $(\pi I)^{-1}$ where I is the resonance intensity. Given that the error in determination of peak width is δv and that the error in measuring peak height is δh , the variance of the estimate for $\Delta v_{1/2}$, $\sigma^2(\Delta v_{1/2})$ is given by

$$\sigma^2(\Delta v_{1/2}) = (\Delta v_{1/2}(\delta h/h))^2 + (\delta v)^2 \quad (5)$$

Plots were made of τ_{ex} vs. $[B]^{-1}$ and the slopes, intercepts (τ_{op}), and their errors computed by using a weighted, least-squares program.

RESULTS

Real-Time Exchange in Intact 5S RNA. Several real-time exchange experiments were conducted on samples of intact 5S RNA by dilution with D₂O buffer at 298 K. Regardless of variations in experimental protocol the results were always the same. The first spectra, which were accumulated within 3 min of addition of D₂O, were identical with spectra taken after 30 min or longer. Difference spectra between early time and late time spectra were flat in the imino proton region. We conclude that both the opening times for 5S RNA base pairs and the exchange times for their imino protons are fast compared to 3 min.

Because imino proton exchange in 5S RNA is too fast to be measured by real-time methods, it was necessary to turn to relaxation techniques in order to obtain quantitative data. The downfield spectrum of intact 5S RNA does not lend itself to studies of this kind, however, because its resonances are broad and the spectrum as a whole is poorly resolved. For this reason, relaxation measurements were made on fragment 1, a large oligonucleotide fragment derived from 5S RNA whose spectrum is much more tractable. Figure 1 shows the sequence of 5S RNA. Fragment 1 comprises bases 1–11 and 69–120 of the 5S sequence. Extensive data exist showing that the structure of fragment 1 is closely related to that of the same sequences in the parent molecule (Kime & Moore, 1983a–c). Figure 2 shows the sequence of fragment 1 and specifies the assignments of downfield resonances as they are currently understood (Kime & Moore, 1983a; Kime et al., 1984; Jarema & Moore, 1986; S. Abo, D. T. Gewirth, N. B. Leontis, and P. B. Moore, unpublished observations). (The reader will find a downfield spectrum for fragment 1 with its resonances named in Figure 3.)

Base-Catalyzed Exchange in Fragment 1. A series of spectra were taken of fragment 1 in the presence of varying concentrations of Tris. Two spectra from the series are shown

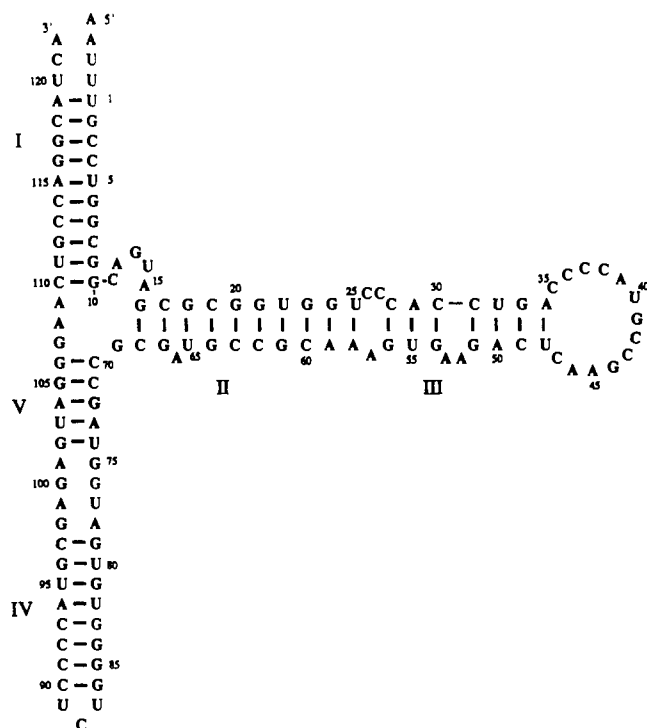


FIGURE 1: The sequence of the 5S RNA from *E. coli* is displayed in the standard three-stem secondary structure [see Delihais et al. (1984)]. The helical stems are designated with Roman numerals.

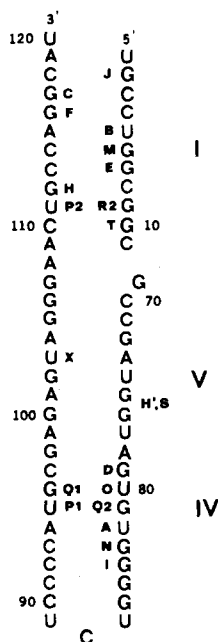


FIGURE 2: The sequence of the fragment 1 portion of 5S RNA is shown. The assignments of downfield imino proton resonances to the sequence are indicated (Kime & Moore, 1983a; Kime et al., 1984; Jarema & Moore, 1986; S. Abo, D. T. Gewirth, N. B. Leontis, and P. B. Moore, unpublished observations). The assignments for resonances H' and S are still not fully settled. ^{15}N labeling data indicate that S is a GN1 imino proton located between bases 69 and 87 in the sequence and that H' is a UN3 proton in the same region. S and H' give mutual NOEs. S is either G75 or G76; H' has to be U74 or U77 (S. Abo, D. T. Gewirth, N. B. Leontis, and P. B. Moore, unpublished data).

in Figure 3, one obtained at 303 K at 0.5 mM and the other in 50 mM Tris at the same temperature. It is clear that addition of Tris to fragment 1 samples has a measurable effect on the line widths of some but not all of its downfield resonances. The broadening of resonances O, P, Q, and some of

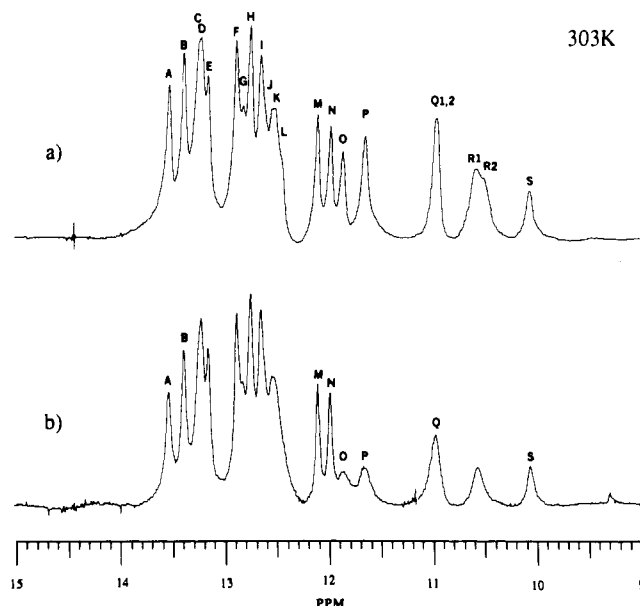


FIGURE 3: The downfield spectrum of fragment 1 is shown at two different Tris concentrations. A 1 mM sample of fragment 1 was prepared in 0.5 mM Tris, 100 mM KCl, and 5 mM MgCl_2 , at pH 7.4. The downfield spectrum of that sample at 303 K is shown in a. Spectrum b is of the same sample following the addition of Tris to bring the Tris concentration to 50 mM. The lettering of the resonances in spectrum a correspond to the assignments given in Figure 2.

the R resonances is conspicuous. The chemical shifts of resonances, however, are not affected by these alterations in tris concentration.

Experiments were also done where KCl was added to samples, not Tris. Resonance line widths did not respond to added KCl over the concentration range used in the Tris addition experiments. Thus the line broadening observed when Tris is added to these samples is not the product of an ionic strength induced change in RNA conformation, consistent with the view that the effect has to do with the catalytic properties of the Tris base.

A troublesome problem in the quantitative analysis of line broadening effects is establishing the width a resonance would have in the absence of exchange under the prevailing conditions. This reference width is subtracted from that observed to estimate the extent of exchange broadening. Several methods for dealing with this problem were examined. The one described below worked reasonably well.

It was found that the line widths of the well-resolved GC resonances M and N were unaffected by addition of Tris, up to a concentration of 200 mM, at all the temperatures studied (293, 303, and 313 K). They are also the narrowest imino proton resonances in the spectrum. The widths of these resonances were taken as representing the widths all imino resonances in the spectrum would have in the absence of exchange. Exchange broadening, $\Delta\nu_{\text{ex}}$, was calculated by subtracting the line width of resonance M (or N) from the line width of all other resonances. Exchange lifetimes, τ_{ex} , were calculated from $\Delta\nu_{\text{ex}}$ for each resonance, and plotted against $1/[\text{buffer}]$. A weighted, linear, least-squares routine was used to extract estimates of τ_{op} and $[\text{B}_{\text{eq}}]$ from each data set. The results are tabulated in Table I.

It will be noted that within the temperature range examined none of the well-resolved GC imino protons was Tris sensitive with the possible exception of J; data are reported in Table I for AU and GU base pairs and for a single, possible AG base pair (resonance S) only. In general, the value of τ_{op} for a given

Table I: Analysis of the Dependence of τ_{ex} on Catalyst Concentration in Fragment 1 in the Presence of Mg^{2+} ^a

resonance	temp (K)	τ_{op} (ms)	$\tau_{op}[B_{eq}]$ (ms M)
A (U82)	293	13.8 (1.9)	0.04 (0.03)
	303	6.9 (1.5)	0.43 (0.11)
	313	3.4 (0.6)	0.22 (0.03)
B (U5)	293	11.4 (4.4)	0.04 (0.03)
	303	16.2 (3.5)	0.39 (0.19)
	313	6.5 (2.5)	0.75 (0.26)
O (U80)	293	3.5 (1.1)	0.30 (0.07)
	303	3.6 (1.4)	0.13 (0.03)
	313	3.5 (1.2)	0.05 (0.01)
P (U95)	293	7.8 (1.6)	0.13 (0.04)
	303	6.0 (1.8)	0.12 (0.03)
	313	5.1 (1.6)	0.04 (0.01)
Q (G81, G96)	293	10.3 (1.0)	0.11 (0.03)
	303	5.9 (0.7)	0.11 (0.02)
	313	4.4 (0.4)	0.07 (0.01)
S	293	19.3 (3.4)	0.0 (0.04)
	303	14.3 (1.8)	0.02 (0.02)
	313	8.4 (0.6)	0.02 (0.01)

^a τ_{ex} vs. base concentration data obtained by the line broadening technique explained under Materials and Methods was analyzed by using eq 3. Reported are τ_{op} , which is the intercept of a plot of τ_{ex} vs. $1/[B]$ extrapolated to infinite base concentration, and $\tau_{op}[B_{eq}]$, which is the slope of the plot. The slope and intercept were obtained from the data by a weighted linear, least-squares algorithm. Standard errors are given after each numerical value (in parentheses). The reference line widths were: at 293 K, 30.1 Hz; at 303 K, 23.9 Hz; at 313 K, 20.6 Hz.

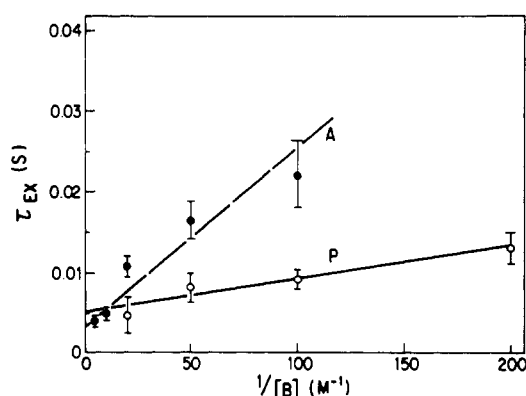


FIGURE 4: A plot of exchange time vs. $[Tris]^{-1}$ is displayed for two resonances, A and P at 313 K in the presence of Mg^{2+} . Exchange times were estimated from resonance widths as described under Materials and Methods. A fragment 1 sample was prepared as described in the legend for Figure 3. Spectra were taken at a series of different Tris concentrations.

resonance decreases with increasing temperature between 293 and 313 K. Opening times depend not only upon base type but to some degree also on the sequence context. The value of τ_{op} for AU resonance B, which has GC base pairs on both sides, is longer than that of resonance A, which represents an AU flanked by a GU and a GC. Similarly, the lifetime of resonance P is longer than that of resonance O. Resonance P belongs to U95, which is located more centrally within helix IV than O, which is assigned to U80. Both protons are involved in GU base pairs.

While the opening times of the AU resonances are not much greater than those of the GU resonances at 303 K, their sensitivities to added Tris are greater. Figure 4 compares the data for resonances A (U82-A94) and P (U95-G81) at 313 K. The implication of the differences in slope is that resonance O will be broader than resonance A at finite catalyst concentration, even though the opening times of the base pairs they represent are similar.

At 293 K the line widths of several of the resonances listed in Table I show little, if any, dependence on added Tris (e.g.,

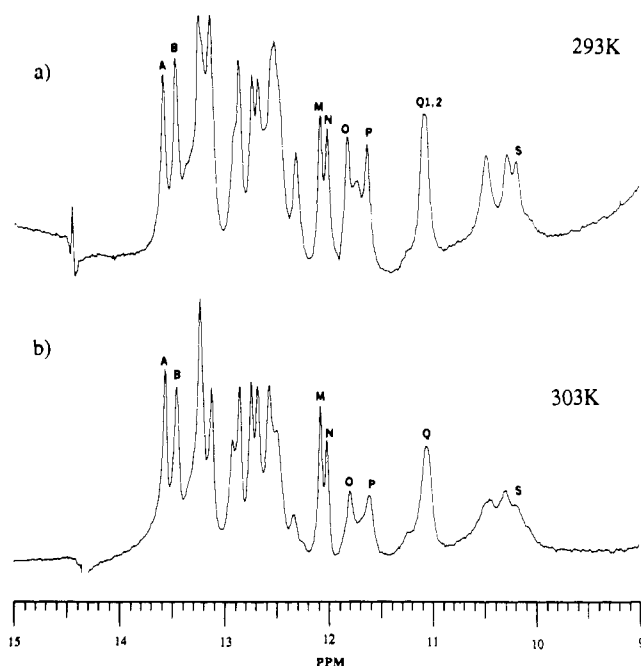


FIGURE 5: The effect of spermidine on the spectrum of fragment 1. A fragment 1 sample was prepared in 0.1 M KCl, 5 mM HEPES, and 1 mM spermidine, at pH 7.2. The spectrum of this sample is shown at 293 (a) and at 303 K (b).

resonances A and S). Plots of τ_{ex} vs. $1/[B]$ are virtually flat for these resonances. These data could mean that τ_{op} is so small that even when the buffer concentration is very high exchange has no effect on line width. In this case, the value obtained for τ_{op} from a flat plot represents error in the reference value for line width. Alternatively, the insensitivity of line width to added buffer could mean that it is an ineffective exchange catalyst for the proton in question for some reason. In the former case the true value of τ_{op} is larger than reported by some indefinite amount, and in the latter case, the values found for τ_{ex} are real, but τ_{op} is being overestimated. Resonance S constitutes a case in point.

S has a line width at low base concentration larger than most other resonances in the spectrum. Its relaxation in the range of 293–313 K includes an important exchange component as judged by T₁ measurements (see below), but its exchange rate does not respond to added Tris; the slope parameters reported in Table I for S are near zero.

The exchange of S appears to be greatly facilitated by 1 mM spermidine. Figure 5 shows spectra of fragment 1 in 1 mM spermidine, 5 mM HEPES, pH 7.2, and 0.1 M KCl (no magnesium) at 293 and 303 K. Exchange broadening of resonances O, P, Q, and R and S in the presence of spermidine is particularly obvious at 303 K. Significant chemical shift changes also accompany the shift to spermidine, however, and some new resonances appear, notably one at about 12.6 ppm and another between O and P at about 11.7 ppm. The change in the exchange properties of S could reflect a specific effect of spermidine on that particular proton or it might equally be due to the spermidine-induced change in RNA conformation to which the chemical shift changes, and the new resonances induced by spermidine bear witness.

T₁ Measurements on Fragment 1. T₁ measurements were done at 283 and 293 K and at every 5 K from 293 up to 333 K on samples in 5 mM cacodylate, a poor exchange catalyst. Before discussing the data, two technical points should be noted. First, prolonged exposure of RNA to high temperatures in the presence of Mg^{2+} leads to phosphate diester hydrolysis. Aliquots were removed from samples after each run and an-

Table II: Analysis of the Dependence of T_1 on Temperature at Low Catalyst Concentration^a

resonance	k_m (Hz)	k_{ex} (Hz)	ΔH (kcal M ⁻¹)
F	10.5 (0.5)	$5.3 (0.3) \times 10^{16}$	23.4 (0.5)
B	10.1 (0.5)	$3.9 (0.4) \times 10^{14}$	19.9 (0.2)
M	8.8 (0.4)	$1.3 (0.1) \times 10^{13}$	18.7 (0.2)
E*	9.4 (0.5)	$2.9 (0.3) \times 10^9$	13.4 (0.2)
H	11.6 (0.6)	$4.3 (0.3) \times 10^{18}$	26.0 (0.2)
S	16.6 (1.0)	$1.5 (0.1) \times 10^{17}$	22.3 (0.1)
O	5.6 (0.5)	$1.4 (0.1) \times 10^{16}$	20.9 (0.1)
Q	7.3 (0.5)	$5.7 (0.3) \times 10^{16}$	22.3 (0.1)
P	8.4 (0.6)	$3.5 (0.2) \times 10^{16}$	21.6 (0.1)
A	10.3 (0.7)	$1.6 (0.1) \times 10^{18}$	23.1 (0.3)
N*	9.1 (0.5)	$7.5 (0.7) \times 10^{10}$	16.6 (0.2)

^a T_1 data collected at different temperatures were fitted to eq 4 as described under Materials and Methods. Values for the three parameters calculated from the fitting procedure are reported along with their standard errors (in parentheses). k_M is the magnetic relaxation rate for a resonance at 20 °C. k_{ex} is the exchange rate at infinite temperature, and ΔH is the activation energy for exchange. Resonances are listed in the order they appear in the sequence with the helix I group above the helix IV, helix V group.

alyzed on native and denaturing acrylamide gels to check for damage. Significant hydrolysis was not observed until after the completion of the 333 K run. Some of the data taken at 333 K has been excluded from analysis.

Second, in order to get useful information from T_1 measurements in this context, the relaxation rates measured for individual resonances must be free of significant "contamination" from cross-relaxation effects (Kearns, 1983). To test whether the semiselective inversion method used was giving good data, the relaxation times of several resonances were measured by selective saturation recovery at 313 K. The decoupler was used to saturate resonances A, M, and O one at a time, and the recovery of these resonances from saturation followed as a function of time. A, M, and O represent an AU, a GC, and a GU imino proton, respectively. (Selective saturation recovery gives reliable data but is far more time consuming than the semiselective method used here which allows all downfield resonances to be measured simultaneously.) The relaxation times obtained by selective saturation recovery were the same as those obtained by semiselective inversion recovery, validating the data obtained in the latter manner. It should also be noted that if the pulse sequence used for semiselective excitation were not working properly, T_1 should decrease with temperature at all temperatures. The fact that T_1 for many resonances increased with temperature at low temperatures in these studies indicates that reasonably selective inversion was achieved (Kearns, 1983).

The relaxation parameters obtained by analyzing the T_1 data as described under Materials and Methods are given in Table II. [Relaxation times for helix IV resonances at different temperatures are tabulated in Leontis et al. (1986a).] Only those resonances are listed which were well enough resolved so that their amplitudes could be accurately determined at all temperatures and which showed appreciable Arrhenius behavior over the temperature range explored. The parameter extraction algorithm fails with data sets which lack a firm indication of the high-temperature trend of T_1 . The data for resonances E and N were marginal in this respect, and the parameters listed for them in Table II are marked with an asterisk. Figure 6 shows plots of the logarithm of the relaxation rate vs. T^{-1} for resonances P and F. The smooth curves are the eq 4 fits to the data. Clearly eq 4 constitutes a plausible model for the relaxation behavior of these resonances.

Once the T_1 parameters are known for a resonance, its imino proton exchange rate can be calculated at any temperature

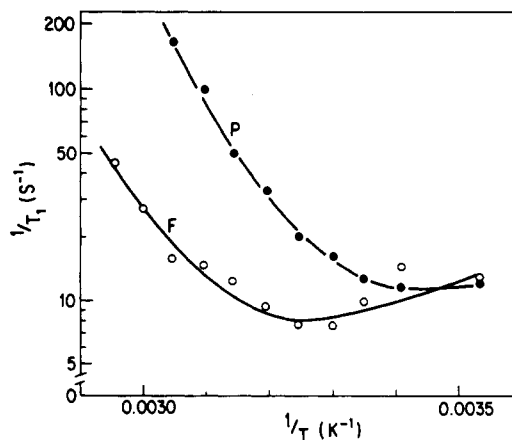


FIGURE 6: An Arrhenius analysis of the temperature dependence of T_1 for resonances P and F. T_1 measurements were made on a fragment 1 sample in 0.1 M KCl, 5 mM MgCl₂, and 5 mM cacodylate, at pH 7.2 and a series of temperatures. Relaxation rates (T_1^{-1}) are plotted against the reciprocal of the absolute temperature. Data are shown for resonances P and F. The smooth curves through the data points represent the best fits of eq 4 to the data.

Table III: Comparison of the Exchange Rates Calculated from Line Broadening with Those Calculated from T_1 Data at 318 K^a

resonance	exchange rates (Hz)		
	318 K, T_2	318 K, T_1	303 K, T_1
F		3.8 (1.5)	0.71
B	11.0 (7.0)	8.7 (1.5)	1.8
M		1.7 (0.4)	0.42
E*		1.8 (0.6)	0.69
H		5.0 (1.9)	0.76
S	79.0 (8.0)	71.0 (12.0)	12.4
O	69.0 (8.0)	60.0 (10.0)	11.7
Q	^b	29.0 (4.0)	5.1
P	56.0 (8.0)	52.0 (9.0)	8.7
A	27.0 (9.0)	24.0 (10.0)	4.1
N*		2.5 (0.8)	0.80

^a Exchange rates were calculated with k_{ex} and ΔH for each resonance at 318 K by using the parameters given in Table II (" T_1 exchange rate"). The T_1 rates are compared with exchange rates estimated from line broadening (" T_2 exchange rate") by using the techniques described for base-catalyzed exchange measurements under Materials and Methods. T_2 exchange rates are given only for those resonances whose line widths increase sufficiently relative to the reference line width (resonance M) to permit accurate estimation of exchange. T_1 rates are also given for 303 K for comparison with τ_{op} values given in Table I. The percentage errors in the estimates at 303 K are about the same as those for 318 K. ^b Resonance Q is a double resonance whose components have chemical shifts which differ slightly. At low exchange rates, its width is not an accurate indicator of exchange.

for the same ionic conditions. These calculated rates should correspond to the rates indicated by line broadening. To find out whether consistent data were being obtained, the spectra acquired in the course of T_1 measurements were analyzed by using the line broadening method, taking the width of resonance M as the reference, as usual. Exchange rates calculated from T_1 relaxation parameters are compared with line broadening exchange rates at 318 K in Table III. Only when the exchange rate exceeds about 10 s^{-1} is there sufficient line broadening to measure with any accuracy. Hence line width observations are reported for only the faster exchanging resonances. The agreement between the calculated and observed rates is good.

Imino Proton Exchange in the L25-Fragment 1 Complex. A useful aspect of the base catalyst method is that it permits exchange measurements to be made without subjecting samples to high temperatures. This fact enabled us to obtain exchange data on L25's complex with fragment 1 which is temperature

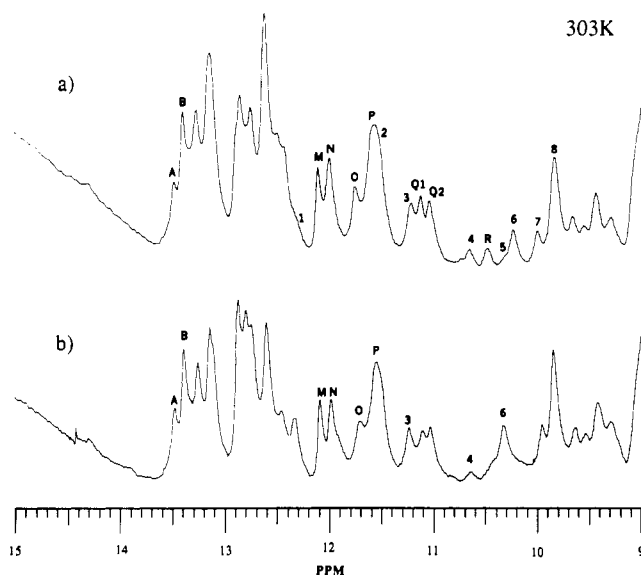


FIGURE 7: The effect of Tris on the downfield spectrum of a fragment 1-protein L25 complex is shown. The sample in question is a stoichiometric complex of fragment 1 and L25 in 0.1 M KCl, 5 mM MgCl_2 , and 5 mM cacodylate, at pH 7.2. Spectrum a is the one observed in the absence of Tris (cacodylate is the buffer), and spectrum b is the result when the Tris concentration is brought to 40 mM under otherwise identical conditions.

Table IV: τ_{op} for Resonances in Fragment 1 in the Presence and Absence of Protein L25 in Mg^{2+} -Containing Buffer at 303 K^a

resonance	τ_{op} (ms)	
	-L25	+L25
B (U5)	16.2 (3.5)	unaff
S	14.3 (3.3)	unaff
Q1 (G96)	5.9 (0.7)	about 3.3
O (U80)	3.6 (1.4)	3.3 (1.0)
P1 (U95)	6.0 (1.8)	unaff
Q2 (G81)	5.9 (0.7)	17.0 (3.0)
A (U82)	6.8 (1.5)	unaff
N (G83)	unaff	unaff
I (G84)	unaff	unaff
2		unaff
3		unaff
6		15.0 (2.5)
8		unaff

^a τ_{op} has been measured for samples of fragment 1 in the presence and absence of L25 at 303K as given under Materials and Methods (see Table I). Resonances are listed in the order in which they appear in the sequence (see Figure 2) starting with helix I at the bottom and finishing with helix IV at the bottom. τ_{op} is reported both in the presence and absence of L25 in ms with standard errors indicated (in parentheses). The designation "unaff" means that the width of the resonance in question does not respond to added Tris. All numbered resonances are unique to the L25 complex and are not observed in fragment spectra in its absence. The reference line width for the spectrum without L25 was 23.9 Hz. The reference for the spectrum in the presence of L25 was 30.0 Hz.

sensitive because L25 denatures at an appreciable rate at room temperature. Figure 7 compares spectra of the L25-fragment complex in 5 mM cacodylate, pH 7.2, in the presence and absence of 40 mM Tris. The lettered resonances in Figure 7 are fragment resonances which retain their identity in the complex. The numbered resonances are unique to the complex. Comparison of Figures 7 and 3 (free fragment, at 0.5 and 50 mM Tris) reveals that the sensitivities of a number of resonances to Tris-catalyzed exchange are substantially reduced by the protein. The results of the numerical analysis of the spectra are presented in Table IV.

Resonances 1, 4, and 5 in the complex are weak and could not be analyzed. Resonance 2 appears as a shoulder on P, and

Table V: τ_{op} for Resonances in Fragment 1 in the Presence and Absence of Protein L25 in Mg^{2+} -Free Buffer at 303 K^a

resonance	τ_{op} (ms)	
	-L25	+L25
B (U5)	6.1 (3.6)	11.4 (3.2)
S	not observed	8.8 (1.6)
O (U80)	3.2 (1.2)	2.8 (0.4)
Q1 (G96)	5.8 (1.0)	3.9 (0.8)
P1 (U95)	4.1 (1.1)	4.8 (0.4)
Q2 (G81)	5.8 (1.0)	8.2 (1.6)
A (U82)	8.4 (1.8)	unaff
N (G83)	unaff	unaff
I (G84)	unaff	unaff
1		not observed
2		7.0 (2.0)
3		not observed
6		not observed

^a τ_{op} was measured on samples of fragment 1 in the presence and absence of L25 under conditions identical with those used for the experiments reported in Table III except that the Mg^{2+} was replaced by 2mM EDTA. For an explanation of this table, see the legend for Table III. The reference line widths for fragment in the absence of L25 was 16.9 Hz. The reference for measurements in its presence was 30.0 Hz.

is also hard to analyze quantitatively. However, neither P nor 2 broadened up to 120 mM Tris. Resonance Q1 is partly overlapped by resonances 3 and Q2. It did broaden in response to added Tris, but the effect could not be accurately quantified. Its behavior is comparable to that of resonance O (see Table III). Q1 and O belong to the G and U imino protons of the same GU base pair (U80-G96). Like resonances P and 2, resonances A, B, 3, and 7 do not respond to added Tris. The values of τ_{op} obtained for resonances Q2 and 6 are around 15 ms, large by the standard of the GU and AU resonances in free fragment.

Increasing the Tris concentration causes some changes in the spectrum of the complex which are not understood. A resonance located at 12.60 ppm in 5 mM cacodylate (pH 7.2) moves progressively downfield as the Tris concentration increases until by 80 mM added Tris it overlaps resonance F at 12.89 ppm. NOE experiments have shown that in the complex at 5 mM cacodylate resonances I and J coincide at 12.60 ppm (Kime & Moore, 1983b). Considering that L25 binds to helix IV, it is likely that the affected resonance is I, but this has not been confirmed by NOE. Another change promoted by increasing the concentration of Tris is an upfield shift of resonances K and L. In contrast to their behavior in free fragment, these as yet unassigned resonances are not significantly broadened by Tris in the L25 complex. Resonances A and B are not measurably broadened by addition of Tris in the complex at 303 K in the presence of Mg^{2+} .

The relaxation properties of the fragment 1-L25 complex were also compared to those of free fragment 1 in buffers lacking Mg^{2+} . The downfield spectrum of fragment 1 is altered appreciably by the removal of Mg^{2+} . Many resonances change their chemical shifts. Some broaden, and others completely disappear. The details of these alterations will be discussed elsewhere (Leontis et al., 1986b) and are not of concern here. Comparing opening times for free fragment in the presence and absence of Mg^{2+} (Tables IV and V), it is clear that the opening times for the resonances which can be observed under both conditions are not particularly sensitive to the cation, with the possible exception of resonance B.

While τ_{op} does not change much with magnesium concentration in fragment 1, the slopes of the τ_{ex} vs. $[\text{B}]^{-1}$ plots one obtains for many resonances do change when magnesium removed from the system. In general they decrease. What this

means is that if spectra are taken of two samples of 5S RNA which are identical except that one has magnesium present and the other does not, the line widths of some of the resonances in the spectrum of the low magnesium sample will be broader than they are in the spectrum of the high magnesium sample. This effect seems to be responsible for the fact that low magnesium spectra look partially "melted" compared to high magnesium samples observed at the same temperature (Leontis et al. (1986a)).

When L25 is added in the absence of Mg^{2+} , many of the same protein stabilization effects seen in the presence of Mg^{2+} recur. Resonance A is rendered insensitive to base. In the absence of L25, A is less stable than B; in the presence of L25, A is more stable than B. S, which is so destabilized by the removal of Mg^{2+} that it cannot be observed, is restored. Resonance 2 behaves similarly. There are two clear differences between the complex in Mg^{2+} and the complex in its absence, however. In the latter case, several of the complex-specific resonances seen in Mg^{2+} are absent. In the presence of Mg^{2+} , L25 stabilizes U95-G81 but not U80-G96. In the absence of the cation, neither GU is stabilized by the protein.

Comparing Tables IV and V the reader will note that the line width of the reference resonance, M, is sensitive to Mg^{2+} ion concentration. At 303 K its width in the presence of the cation was about 24 Hz; in the absence of the cation the width was about 17 Hz. We have noticed in the past that as the RNA concentration in fragment 1 samples increases past 1 mM in magnesium-containing buffers that downfield resonances broaden, suggesting aggregation. Since magnesium promotes nucleic acid aggregation, it is not surprising that its removal from these samples reduces resonance line widths.

DISCUSSION

The real-time exchange experiments on intact 5S RNA were carried out under buffer conditions which discourage exchange (5 mM cacodylate, pH 6.0). Nevertheless, no slowly exchanging imino protons were observed. This contrasts with the behavior of many tRNAs. Leroy et al. (1985a) have reviewed the data on slowly exchanging imino protons in various tRNAs. For yeast tRNA^{Phe} they report four imino protons which exchange slowly enough to be observed in real-time experiments. Three of these resonances have been assigned to GC base pairs in the dihydrouracil stem. Slow exchange in tRNA is not limited to GCs, however. It appears that 5S RNA is not as rigid a molecule as tRNA.

Proton exchange has been studied in 5S RNA by tritium exchange methods (Ramstein & Erdmann, 1981). The tritium exchange data support the view that 5S RNA has a "looser" structure than tRNAs in general. No protons in 5S RNA exchange with half-times greater than tens of minutes; in tRNAs there are small numbers of protons with exchange times of many hours. Tritium exchange experiments do not distinguish one class of protons from another; they provide only a lower bound for what the exchange rate of imino protons might be in 5S RNA.

As Gueron and his co-workers have pointed out, their data demonstrating the sensitivity of imino proton exchange rates to catalyst concentration raises questions about the interpretation of much of the downfield T_1 data in the NMR literature on nucleic acids. It appears that many of the experiments reported cannot have given reliable information about base pair opening rates because they were done under exchange-limited conditions (Leroy et al., 1985a,b). The Arrhenius activation energies which emerge from the T_1 data discussed here (see Table II) support this contention. All imino protons have the same activation energy for exchange, about 20

kcal/mol. Values in this range are typical for experiments of this kind [e.g., Mirau et al. (1985)]. The constancy of these activation energies from one base pair to the next suggests that they relate to the chemistry of exchange, which is the same for all base pairs, not the opening process which should vary from one base pair to the next. (Note that Table II has data for GC, AU, and GU base pairs as well as a possible AG base pair.)

Were one to collect data on τ_{op} for a set of resonances at several temperatures, an Arrhenius analysis should provide estimates for the activation energy of the base pair opening process. The data in Table I do not run over a wide enough temperature range to permit accurate estimates to be made. It is nevertheless interesting to see what the data suggest. The apparent activation energies for resonances A, P, O, and Q, the only ones for which the data are at all persuasive, are as follows: A, 12.7 kcal M⁻¹; P, 3.8 kcal M⁻¹; O, essentially zero; Q, 6.8 kcal M⁻¹. As expected, there are big differences between base pairs of different kinds. GU base pairs are easier to open than AUs by a large amount, and the UN3 protons in GUs seem to be more "vulnerable" than the GN1s. Clearly further experiments of this kind would be useful.

While measurement of line broadening as a function of catalyst concentration can give kinetic information about helix breathing, it clearly has limitations. If a catalyst causes a resonance to broaden, the analysis works, and an estimate for τ_{op} emerges. If the resonance does not respond, no firm conclusion can be drawn, as pointed out above. In resonance S we have a case of a resonance which is clearly exchanging at room temperature by T_1 criteria but which responds only weakly to added Tris. The data suggest, but do not prove, that Tris simply does not "work" for S. Ambiguities of this kind make it impossible to suggest lower bound limits for τ_{op} for the several resonances in the spectrum of fragment which did not respond to added Tris. Most of them are GCs. All of them disappear from the downfield spectrum if the temperature is raised high enough, indicating that exchange is possible. Thus it is plausible to suggest that τ_{op} is quite large for these resonances, greater than 20 ms, but the data are not conclusive.

It is conceivable that the resonance broadening effects reported above might reflect structural changes in the RNA induced by the catalyst being added. Were this the case, the interpretation of the data in terms of exchange would clearly be misleading. This alternative explanation of the data cannot be excluded categorically, but we think it implausible. First, Leroy et al. (1985a) have demonstrated in a number of cases that the value found for τ_{op} for a given imino proton is independent of the substance used to catalyze exchange. This finding shows that at least some of the time, τ_{op} is a property of the molecule, not the catalyst used. Second, our own data shown that the line-broadening effects reported above for 5S RNA are not reflections of the increase in ionic strength which accompany the addition of catalyst to the sample. Third, the chemical shifts of the resonances which are broadened by the addition of Tris are not altered by it. The chemical shifts in 50 or 10 mM Tris, a good exchange catalyst, are the same as the chemical shifts in 5 mM cacodylate, a poor exchange catalyst. It is unlikely that the addition of Tris to the system alters its structure. Fourth, the data obtained with spermidine provide an example of a catalytically effective substance which clearly does alter the structure of the RNA. In that case chemical shifts change, and new resonances appear, signaling the fact that a conformational change has taken place.

Once the problems of interpreting imino proton exchange data in terms of helix dynamics are recognized, some ambi-

guities inherent in the interpretation of NMR downfield melting data must be acknowledged. In an NMR melting experiment done on the downfield spectrum of a nucleic acid, what is being observed the resistance of resonances to exchange as a function of temperature. Given the complexities that surround exchange, the resistance of a given resonance to exchange cannot necessarily be equated with thermodynamic stability of the base pair of which it is a part. It is clear that melting data should be collected with a buffer concentration series run at each temperature.

It is in this same light that the data on the influence of L25 binding have to be interpreted. It is clear that L25 reduces the rate of exchange of a large number of resonances in fragment 1. These reductions in exchange rate are confined primarily to resonances whose chemical shifts are perturbed by L25 binding. Not all resonances which "feel" L25 by the criterion of chemical shifts are affected, however. Resonances O and Q1 do "feel" the effect of L25 as judged by chemical shift (Kime & Moore, 1983b), but their opening times do not change. On the other hand, the downfield resonances induced by L25 binding, many of which most likely to not represent normal base pairs, are insensitive to added Tris in the presence of Mg^{2+} . Since almost none of the stabilized resonances shows an appreciable buffer effect, it is not possible to calculate opening rates for them. It follows from the discussion above that the simplest explanation one could imagine for these data, that L25 binding stabilizes the secondary structure of its binding site, is supported but not proven by these data. Only in the case of resonance Q2 (G81) whose opening time is measurable both in the presence and absence of the protein can a firm conclusion be reached. For that one resonance, stabilization is proven; its opening time is increased almost threefold when L25 binds.

ACKNOWLEDGMENTS

We are indebted to Drs. A. G. Redfield and M. Gueron for sharing with us their insights into imino proton exchange. We thank Betty Freeborn and Grace Sun for the able technical assistance they have provided. We are indebted to Peter Demou for facilitating the NMR spectroscopy.

Registry No. Adenine, 73-24-5; guanine, 73-40-5; uracil, 66-22-8.

REFERENCES

- Aylward, N. N. (1967) *J. Chem. Soc. B*, 401-403.
 Bard, Y. (1974) *Non-Linear Parameter Estimation*, Academic, New York.
 Brosius, J. (1984) *Gene* 27, 161-172.
 Cantor, C. R., & Shimmel, P. R. (1980) *Biophysical Chemistry*, W. H. Freeman, San Francisco.
 Delhas, N., Anderson, J., & Singhal, R. P. (1984) *Prog. Nucleic Acid Res. Mol. Biol.* 31, 161-190.
 Eigen, M. (1964) *Angew. Chem., Int. Ed. Engl.* 3, 1-19.
 Englander, S. W., & Kallenbach, N. R. (1983) *Q. Rev. Biophys.* 16, 521-655.
 Fritzsche, H., Kan, L.-S., & Ts'o, P.O.P. (1981) *Biochemistry* 20, 6118-6122.
 Hurd, R. E., & Reid, B. R. (1980) *J. Mol. Biol.* 142, 181-193.
 Jarema, M., & Moore, P. B. (1986) in *3D Structure and Dynamics of RNA* (van Knippenberg, P. H., Ed.) Plenum, New York.
 Kearns, D. R. (1983) *CRC Crit. Rev. Biochem.* 15, 237-290.
 Kearns, D. R., & Shulman, R. G. (1974) *Acc. Chem. Res.* 7, 33-39.
 Kime, M. J., & Moore, P. B. (1982) *Nucleic Acids Res.* 10, 4973-4983.
 Kime, M. J., & Moore, P. B. (1983a) *FEBS Lett.* 153, 199-203.
 Kime, M. J., & Moore, P. B. (1983b) *Biochemistry* 22, 2615-2622.
 Kime, M. J., & Moore, P. B. (1983c) *Biochemistry* 22, 2622-2629.
 Kime, M. J., Ratcliffe, R. G., Moore, P. B., & Williams, R. J. P. (1981) *Eur. J. Biochem.* 116, 269-276.
 Kime, M. J., Gewirth, D. T., & Moore, P. B. (1984) *Biochemistry* 23, 3559-3568.
 Leontis, N. B., Ghosh, P., & Moore, P. B. (1986a) in *Biomolecular Stereodynamics IV. Proceedings of the Fourth Conversation in the Discipline of Biomolecular Stereodynamics* (Sarma, R. H., & Sarma, M. H., Eds.) pp 287-306, State University of New York, Albany, NY, June 4-9, 1985, Adenine, Guilderland, NY.
 Leontis, N. B., Ghosh, P., & Moore, P. B. (1986b) *Biochemistry* (submitted for publication).
 Leroy, J. L., Bolo, N., Figueroa, N., Plateau, P., & Gueron, M. (1985a) *J. Biomol. Struct. Dyn.* 2, 915-939.
 Leroy, J. L., Broseta, D., & Gueron, M. (1985b) *J. Mol. Biol.* 184, 165-178.
 Marshall, A. G., & Smith, J. L. (1980) *Biochemistry* 19, 5955-5959.
 Mirau, P. A., Behling, R. W., & Kearns, D. R. (1985) *Biochemistry* 24, 6200-6211.
 Patel, D. J., Kozlowski, S. A., Weiss, M., & Bhatt, R. (1985) *Biochemistry* 24, 936-944.
 Ramstein, J., & Erdmann, V. A. (1981) *Nucleic Acids Res.* 9, 4081-4088.
 Roth, K., Kimber, B. J., & Feeney, J. (1980) *J. Magn. Reson.* 41, 302-309.
 Tropp, J. S., & Redfield, A. G. (1983) *Nucleic Acids Res.* 11, 2121-2134.